The Interaction of Symmetric and Asymmetric Modes with Free Electrons in a Traveling-Wave Amplifier

Samer Banna, Levi Schächter and David Schieber
Department of Electrical Engineering
Technion - Israel Institute of Technology
Haifa 32000, Israel

September 7, 2000

Abstract

A 3D model has been developed for the investigation of the coupling of the lowest symmetric and asymmetric modes in a high-power (>50MW), high-efficiency traveling-wave amplifier. It was shown that due to the interaction, the radius of the beam increases linearly with the power associated with the asymmetric mode at the input end. For a specific set of parameters simulations indicate that 0.5MW of HEM_{11L} power at the input end is sufficient to deflect to the wall a beam of 300A/0.85MV guided by a 0.5-1.5T magnetic field. As the existance of an asymmetric mode is therefore impairing the performance of the amplifier, a way to suppress the asymmetric mode is described.

INTRODUCTION

Traveling-wave amplifiers, are widely used as high power microwave sources operating at high frequency. In these amplifiers the main goal is to obtain high efficiency for the main interacting mode. So far, it was assumed that the electron beam interacts with the lowest symmetric TM mode i.e. TM_{01}. Efficiencies as high as 70% and even higher [1] may be achieved in coupled cavity traveling-wave structures, driven by a relativistic, bunched beam, when high order modes do not play a significant role. However, asymmetry may occur due to either the input or output arm, due to uneven azimuthal electron distribution or due to beam misalignment; as a result asymmetric modes may develop. In such a case, a longitudinally modulated beam may interact with one of the asymmetric modes. The main problem with these modes is their ability to deflect the beam to the wall because of their non-zero transverse magnetic field on axis. This phenomenon may be more crucial in traveling-wave amplifier operating at the Ka-band than one operating at the X-band [2], since the former internal radius is smaller than the latter i.e. the gap between the beam outer radius and the structure's wall is smaller. However, beam power requirements and technological constraints push the internal radius of the structure upwards such that when comparing the vacuum wavelength with a practical internal radius, one may found that at Ka-band this radius is larger than the simple frequency scaling criterion dictates.

Since pulse shortening was observed experimentally in high-power traveling-wave amplifier operating at 35GHz as reported by Wang *et. al.* [3], this study investigates the impact of asymmetric modes on the interaction process in a traveling-wave amplifier operating at both bands X and Ka. The build up of asymmetric modes as a very narrow bunch traverses an acceleration structure is understood. But there is no equivalent analysis corresponding to a traveling-wave amplifier where the longitudinal bunch is of the order of the wavelength. Moreover, its transverse size is several order of magnitudes larger in the amplifier case comparing to an accelerator, and collective effects play a dominant role in the former.

In this study the main aspects associated with the operation of high-power traveling-wave amplifier operating at 9GHz and 35GHz, taking into consideration the asymmetric modes are analyzed. Some of the electromagnetic "cold" characteristics of symmetric and asymmetric modes are investigated, followed by introducing the 3D model developed for the investigation of the coupling of symmetric and asymmetric modes and their interaction with an electron beam injected into a traveling-wave amplifier. Specifically, the beam blow up is presented. Finally a way to suppress asymmetric modes is suggested.

PASSIVE SYSTEM ANALYSIS

A uniform beam or initially bunched beam, generated by either a series of cavities (klystron) or a slow wave structure, is injected into a uniform periodic structure as the one illustrated in Figure 1. In order to achieve efficient beam-wave interaction, the structure must be designed so that the main interacting mode i.e. the lowest symmetric mode TM_{01} is synchronized with the electron beam and the interference of asymmetric modes is minimal. Accordingly, one has to investigate firstly the electromagnetic "cold" characteristics of symmetric and asymmetric modes that may propagate in such a structure when no electrons are injected i.e. *passive system* and afterward, the *active system* may be investigated, analyzing the dynamics of the electrons due to their interaction with both symmetric and asymmetric modes.

The first step in understanding the role of asymmetric modes in the interaction process is to investigate their "cold" characteristics. To do so, first, the relation between the mode's wave-number and the operating frequency of the system should be found. Such a relation is called the *dispersion relation.*

Assuming that all the modes within the structure propagate in the z direction, the functional variation of the electromagnetic field components, satisfying the homogeneous wave equation, in the longitudinal and azimuthal direction is known. Moreover, assuming that the system operates in a steady state ($e^{j\omega t}$) and that it remains in a linear regime at all times, all the components of the electromagnetic field, in the internal region ($r < R_{\text{int}}$) of the structure, may be derived from the longitudinal components given by

$$\begin{pmatrix} E_z \\ H_z \end{pmatrix} = \sum_{n,\nu=-\infty}^{\infty} \begin{pmatrix} \mathcal{E}_{n,\nu} \\ \mathcal{H}_{n,\nu} \end{pmatrix} e^{j\omega t - k_n z - j\nu\phi} \mathrm{I}_\nu \left(\Gamma_n r\right), \tag{1}$$

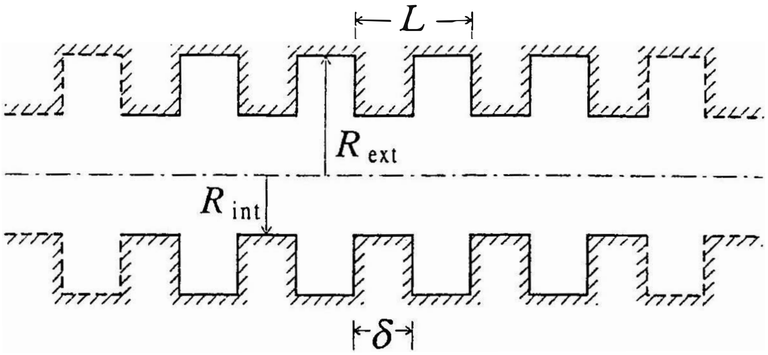

Figure 1: Typical configuration of traveling-wave structure. R_{int}, R_{ext} are the internal and external radii respectively. L is the structure periodicity and δ is the disk thickness.

where $k_n = k + 2\pi n/L$, $|k| < \pi/L$, $\Gamma_n = \sqrt{\left|k_n^2 - \left(\frac{\omega}{c}\right)^2\right|}$ and $\mathrm{I}_\nu(\xi)$ is the modified Bessel function of the first type and order ν. By satisfying the boundary condition at the interface $r = R_{\text{int}}$ the dispersion relation is deduced. In a matrix form the dispersion relation may be written as follows

$$\begin{bmatrix} D^{\mathrm{TM}}(\nu) & C_{12}(\nu) \\ C_{21}(\nu) & D^{\mathrm{TE}}(\nu) \end{bmatrix} \cdot \begin{bmatrix} \mathcal{E} \\ \mathcal{H} \end{bmatrix} = 0. \tag{2}$$

In principle, the matrices D^{TM}, D^{TE}, C_{12} and C_{21}, are infinite. The above notation is convenient, since in the case of symmetric modes ($\nu = 0$) the coupling matrices $(C_{12}(\nu), C_{21}(\nu))$ are identically zero and this equation has two *uncoupled* solutions $\mathrm{Det}\left(D^{\mathrm{TM}}(\nu)\right) = 0$ and $\mathrm{Det}\left(D^{\mathrm{TE}}(\nu)\right) = 0$ that represent all the symmetric transverse magnetic (TM) and transverse electric (TE) modes, respectively. For any other value of ν the coupling matrices are not zero, and as a result, the non-trivial solution of (2) implies that each eigen-mode is a superposition of the two modes (TM & TE). Such modes are called hybrid electric and magnetic modes (HEM). From the perspective of the interaction with the electrons, the main problem with such modes is the fact that they have non-zero magnetic field on axis and consequently, electrons may be deflected to the wall [4-6].

Similar to the symmetric modes, for each radial number ν there are two modes for each asymmetric mode, only that, here, one can no longer distinguish between TM and TE, rather they are referred to as "lower" and "higher" modes. Figure 2 illustrates the dispersion relation of all the modes up to 20GHz of two structures. In the left frame the internal radius of the disk is relatively small (8mm), so that the lowest symmetric mode TM_{01} and the lower branch of the lowest asymmetric mode HEM_{11L} are well separated and do not intersect. The right frame illustrates the case when the latter modes intersect since the internal radius is large (13mm) and, as a result the modes are close to each other. In both cases the structure was designed to operate at 9GHz with a phase advance per cell of $\pi/2$ and phase velocity of $0.933c$; the disk thickness is 1.5mm and the structure periodicity is 7.775mm. As may be concluded from Figure 2, the first mode above the TM_{01}, is the HEM_{11L} , the curves of other modes are far enough from that of the TM_{01} mode. For this reason the first candidate mode to interact with the electron beam, after the main interacting mode TM_{01}, is the HEM_{11L} mode. The overlap between the latter two modes increases when increasing the internal radii. Furthermore, up scaling the operating frequency the overlap increases too [2], so that at Ka-band (35GHz) for any typical value of $R_{\rm int}$ the curve of HEM_{11L} mode intersect that of the TM_{01} mode.

In addition to the dispersion relation there are many other "cold" parameters that affect the interaction process. One of these parameters that may be critical in the design of a slow wave structure is the group velocity of the interacting modes, specially of the HEM_{11L} mode. If the latter is negative an inherent positive feedback develops in the system and the system will oscillate. Obviously, such a case is undesirable in an amplifier. This problem is in particular vital in tapered structures where even if initially the system was designed for a positive group velocity, as the phase velocity of the TM_{01} mode is reduced, the group velocity of the HEM_{11L} mode may become negative. Increasing the internal radius eliminates the positive feedback but it also reduces the interaction impedance; the later is defined as follows

$$\begin{aligned} Z_{\rm int}^{(\rm TM_{01})} &\equiv \frac{1}{2}\frac{\pi R_{\rm int}^2}{P^{(\rm TM_{01})}}\left|\mathcal{E}_{n=0,\nu=0}\right|^2 , \\ Z_{\rm int}^{(\rm HEM_{11\mathit{L}})} &\equiv \frac{1}{2}\frac{\pi R_{\rm int}^2}{P^{(\rm HEM_{11\mathit{L}})}}\left|\mathcal{E}_{n=0,\nu=1}\right|^2 , \end{aligned} \tag{3}$$

where P is the total average power which flows in the system in the specific mode. The interaction impedance is indicative of the electric field that an electron beam experiences as it traverses the structure.

The purpose behind the passive system investigation was to list the main limitations and considerations that must be taken into account when designing traveling-wave amplifier in

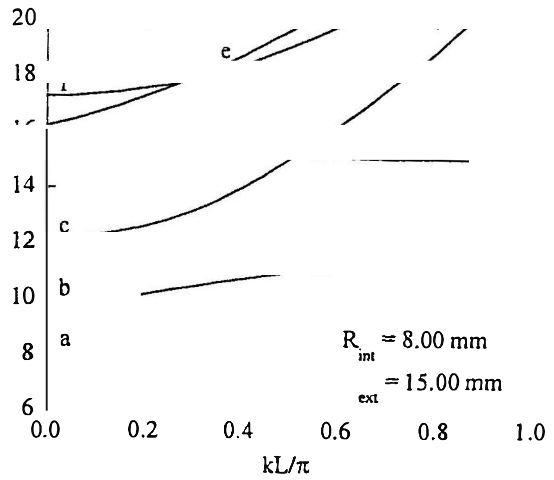

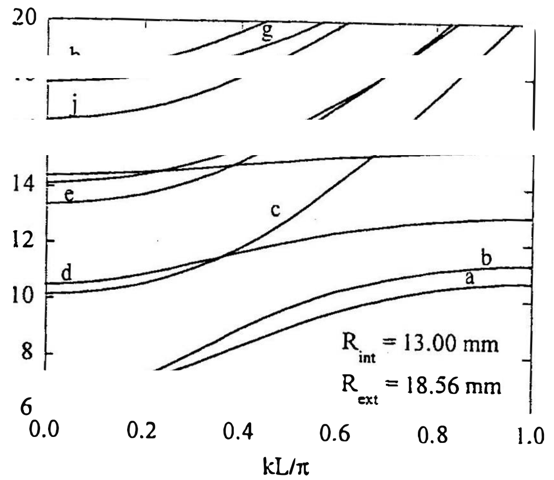

Figure 2: The dispersion relation of all modes up to 20GHz, for two different structures. The legend of the modes: a-TM_{01}, b-HEM_{11L}, c-HEM_{11H}, d-HEM_{21L}, e-HEM_{21H}, f-TM_{02}, g-HEM_{12L}, h-HEM_{12H}, i-HEM_{31L}, j-HEM_{31H}.

order to achieve maximum efficiency via the main interacting mode TM_{01} with minimum interference of the asymmetric modes especially the HEM_{11L} mode. As may be concluded from the discussion above and further investigation (see Ref. 2) the latter two statements conflict each other and a compromise must be made. For system operating at X-band a choice of internal radius in the range of 7.5 – 8.5mm seems to be adequate, since for higher radii modes overlap, whereas for smaller values the group velocity of the HEM_{11L} mode may be negative. While in the Ka-band internal radius of 3.5mm is a reasonable choice.

ACTIVE SYSTEM ANALYSIS

In order to investigate the impact of the HEM_{11L} mode on the interaction process, a 3D quasi-analytic macro-particle model is developed. Within the framework of this model, the full 3D motion of the particles is calculated. However, their effect on the electromagnetic field is assumed to be only in the longitudinal direction (1D). Additional assumptions of the model include: positive group velocity of both modes (TM_{01} & HEM_{11L}), their basic functional form is preserved, the energy conversion is primarily controlled by the longitudinal motion and no electrons are reflected.

The total electromagnetic field propagating along the structure, is composed of three components, the rf field, the dc collective field (space-charge) and the guiding magnetic field B_0 necessary for beam confinement. Bearing in mind that the system operates in steady state, assuming that it remains in a linear regime at all times, using Poynting's theorem and the Newtonian equation of motion for the description of the particles dynamics, the governing equations of the model read

$$
\begin{aligned}
&\frac{d}{d\xi}\left(\frac{a_1}{\sqrt{\alpha_1}}\right) = \sqrt{\alpha_1}\left\langle \mathrm{I}_0(\bar{\Gamma}_1\bar{r}_i)\, e^{-j\chi_{i,1}}\right\rangle_i , \quad \frac{d}{d\xi}\left(\frac{a_2}{\sqrt{\alpha_2}}\right) = \sqrt{\alpha_2}\left\langle \mathrm{I}_1(\bar{\Gamma}_2\bar{r}_i)\, e^{-j\chi_{i,2}+j\phi_i}\right\rangle_i , \\
&\frac{d}{d\xi}\chi_{i,1} = \frac{\Omega_1}{\beta_{z,i}} - K_1 , \qquad \frac{d}{d\xi}\chi_{i,2} = \frac{\Omega_2}{\beta_{z,i}} - K_2 , \\
&\frac{d}{d\xi}\gamma_i = -\tfrac{1}{2}\left[a_1\mathrm{I}_0(\bar{\Gamma}_1\bar{r}_i)\, e^{j\chi_{i,1}} + a_2\mathrm{I}_1(\bar{\Gamma}_2\bar{r}_i)\, e^{j\chi_{i,2}-j\phi_i} + c.c\right] , \\
&\frac{d}{d\xi}\bar{x}_i = \frac{\beta_{x,i}}{\beta_{z,i}} ; \qquad \frac{d}{d\xi}\bar{y}_i = \frac{\beta_{y,i}}{\beta_{z,i}} \\
&\frac{d}{d\xi}\bar{p}_{x,i} = -\Omega_c\frac{\bar{p}_{y,i}}{\bar{p}_{z,i}} + \Omega_p^2\frac{x_i}{2\gamma_{z,i}^2\beta_{z,i}} + \frac{F_x^{(\mathrm{rf})}}{\beta_{z,i}} , \quad \frac{d}{d\xi}\bar{p}_{y,i} = \Omega_c\frac{\bar{p}_{x,i}}{\bar{p}_{z,i}} + \Omega_p^2\frac{\bar{y}_i}{2\gamma_{z,i}^2\beta_{z,i}} + \frac{F_y^{(\mathrm{rf})}}{\beta_{z,i}} , \\
&\bar{p}_{z,i} = \sqrt{\gamma_i^2 - \bar{p}_{x,i}^2 - \bar{p}_{y,i}^2} .
\end{aligned}
\tag{4}
$$

In this set of equations the first line includes the amplitude dynamics equations, followed by the phase dynamics equations and the single particle energy conservation, the last three lines represent the dynamics equations of the particles transverse motion and their normalized momentum $\bar{p}_{x,i} \equiv \gamma_i\beta_{x,i}$, $\bar{p}_{y,i} \equiv \gamma_i\beta_{y,i}$ and $\bar{p}_{z,i} \equiv \gamma_i\beta_{z,i}$ where $\gamma_i = \left(1 - \vec{\beta}\right)^{-1/2}$. Indices 1 and 2 represent the TM_{01} and HEM_{11L} modes correspondingly; $\langle ... \rangle$ represents averaging over entire ensemble of particles. The other definitions used here are $\xi \equiv z/d$, $\bar{x} \equiv x/d$, $\bar{y} \equiv y/d$, $\bar{r} \equiv r/d$, d is the total interaction length, ϕ_i is the azimuthal location of the i'th particle; $\Omega \equiv \omega d/c$, $\Omega_c = ecB_0d/mc^2$, $\Omega_p^2 \equiv \dfrac{C\eta_0}{mc^2/e}\dfrac{d^2}{\pi R_{\mathrm{beam}}^2}\dfrac{1}{\beta_{ph}}$, I is the average current of the electron beam, R_{beam} is the radius of the beam at the input where it was injected and β_{ph} is the phase velocity of both modes, $K \equiv kd$, $\bar{\Gamma} \equiv \sqrt{K^2 - \Omega^2}$, $a \equiv e\mathcal{E}\, d/mc^2$, $\mathcal{E}$ is the amplitude of the zero's harmonic ($n = 0$) of the appropriate mode; $\chi_{i,1}$ is the phase of the i'th particle relative to the TM_{01} mode whereas $\chi_{i,2}$ is the phase of the same particle relative to the HEM_{11L} mode; α_1 and α_2 are the coupling coefficients defined as $\alpha_\mu \equiv \dfrac{IZ_{\mathrm{int}}^{\mu}}{mc^2/e}\dfrac{d^2}{\pi R_{\mathrm{int}}^2}$,

$\mu = 1, 2$. The normalized rf forces calculated using Lorentz law are given by

$$\begin{aligned}
\overline{F}^{(\mathrm{rf})}_{x,i} \equiv \frac{F^{(\mathrm{rf})}_x d}{mc^2} &= A\left\{\left[\dot{\mathrm{I}}_0\left(\overline{\Gamma}_1\overline{r}_i\right)\mathrm{Re}\left(ja_1 e^{j\chi_{i,1}}\right) + \dot{\mathrm{I}}_1\left(\overline{\Gamma}_2\overline{r}_i\right)\mathrm{Re}\left(ja_2 e^{j\chi_{i,2}-j\phi_i}\right)\right]\cos(\phi_i)\right. \\
&\qquad \left. -\frac{\mathrm{I}_1(\overline{\Gamma}_2\overline{r}_i)}{\overline{\Gamma}_2\overline{r}_i}\mathrm{Re}\left(a_2 e^{j\chi_{i,2}-j\phi_i}\right)\sin(\phi_i)\right\} \\
&+ B\left\{\left[\frac{\mathrm{I}_1(\overline{\Gamma}_2\overline{r}_i)}{\overline{\Gamma}_2\overline{r}_i}\mathrm{Re}\left(ja_2 e^{j\chi_{i,2}-j\phi_i}\right)\right]\cos(\phi_i)\right. \\
&\qquad \left. -\dot{\mathrm{I}}_1\left(\overline{\Gamma}_2\overline{r}_i\right)\mathrm{Re}\left(a_2 e^{j\chi_{i,2}-j\phi_i}\right)\sin(\phi_i)\right\}
\end{aligned}$$

$$\begin{aligned}
\overline{F}^{(\mathrm{rf})}_{y,i} \equiv \frac{F^{(\mathrm{rf})}_y d}{mc^2} &= A\left\{\left[\dot{\mathrm{I}}_0\left(\overline{\Gamma}_1\overline{r}_i\right)\mathrm{Re}\left(ja_1 e^{j\chi_{i,1}}\right) + \dot{\mathrm{I}}_1\left(\overline{\Gamma}_2\overline{r}_i\right)\mathrm{Re}\left(ja_2 e^{j\chi_{i,2}-j\phi_i}\right)\right]\sin(\phi_i)\right. \\
&\qquad \left. +\frac{\mathrm{I}_1(\overline{\Gamma}_2\overline{r}_i)}{\overline{\Gamma}_2\overline{r}_i}\mathrm{Re}\left(a_2 e^{j\chi_{i,2}-j\phi_i}\right)\cos(\phi_i)\right\} \\
&+ B\left\{\left[\frac{\mathrm{I}_1(\overline{\Gamma}_2\overline{r}_i)}{\overline{\Gamma}_2\overline{r}_i} : \mathrm{Re}\left(ja_2 e^{j\chi_{i,2}-j\phi_i}\right)\right]\sin(\phi_i)\right. \\
&\qquad \left. +\dot{\mathrm{I}}_1\left(\overline{\Gamma}_2\overline{r}_i\right)\mathrm{Re}\left(a_2 e^{j\chi_{i,2}-j\phi_i}\right)\cos(\phi_i)\right\}
\end{aligned} \tag{5}$$

where $A = -\gamma_{ph}(1 - \beta_{z,i}\beta_{ph})$; $B \equiv jh_0\gamma_{ph}(\beta_{z,i} - \beta_{ph})$ and $h_0 \equiv \eta_0\mathcal{H}_2/\mathcal{E}_2$ where η_0 is the impedance of a plane wave in vacuum.

SIMULATION RESULTS AND DISCUSSION

The first step in analyzing the operation of traveling-wave amplifier at 35GHz, taking into consideration the impact of the asymmetric mode HEM_{11L}, is to compare its performance with the latter turned "on" and "off". The extent the HEM_{11L} mode is destructive is determined in terms of effective radius of the beam defined as $\bar{r}_e \equiv R_e/R_{\mathrm{int}} = 2(d/R_{\mathrm{int}})\left\langle \bar{r}_i \right\rangle_i$. Figure 3 shows the effective radius of the beam's envelope of a structure driven by uniform beam that interact with a TM_{01} mode wave that was injected into the structure, its power level at the input end is assumed to be 5kW. In the left frame the guiding magnetic field is $\mathrm{B}_0 = 0.5$T while in the right frame it is $\mathrm{B}_0 = 1.5$T . Each frame consists of two curves describing the effective radius of the beam for both cases, when the HEM_{11L} mode is turned "off" and "on", where in the latter case its power at the input end is 0.5MW. Bearing in mind that the structure is tuned to allow the symmetric mode leaves the system but not necessarily the asymmetric mode and since a realistic beam pulse lasts for several hundreds

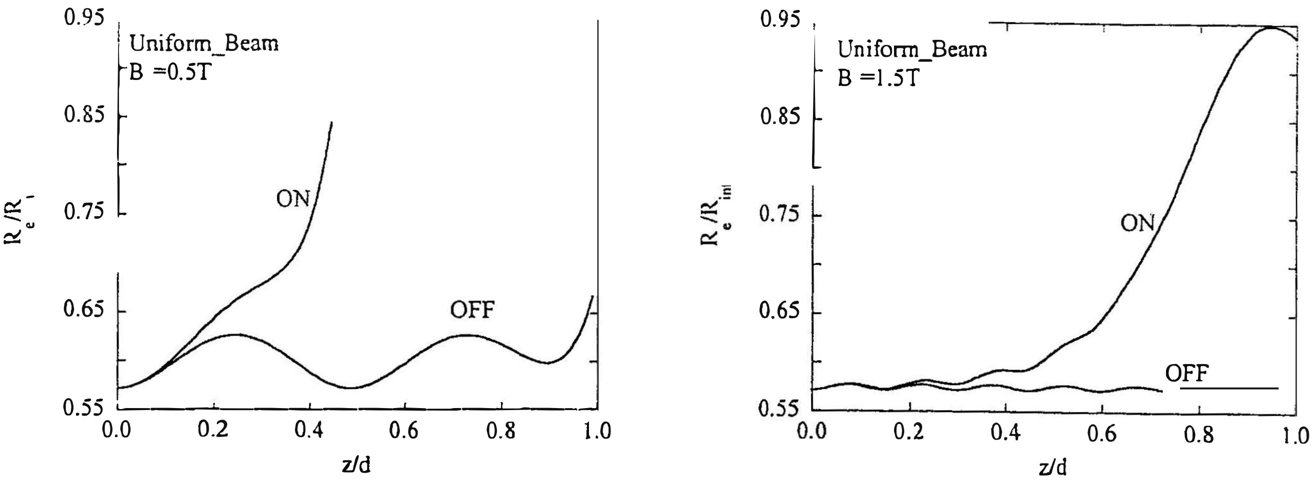

Figure 3: The effective radius of the beam's envelope for both case: HEM_{11L} turned "off" and "on".

of nano-seconds, and there is time for several thousands of round-trips for the asymmetric mode along the structure. As a result the, the asymmetric mode starts to bounce between the two ends of the structures. Accordingly the asymmetric mode power level increases. For this reason the power level of the asymmetric mode at the input end was chosen higher than that of the symmetric mode. The simulation results presented here examines closely the interaction during a single-pass along the structure. The parameters used in this simulation are: $I = 300\mathrm{A}$, $V = 850\mathrm{kV}$, $R_{\mathrm{int}} = 3.5\mathrm{mm}$, $R_{\mathrm{ext}} = 5\mathrm{mm}$, $R_{\mathrm{beam}} = 2\mathrm{mm}$, $L = 1.98\mathrm{mm}$, $f_{\mathrm{TM}_{01}} = 35\mathrm{GHz}$, $f_{\mathrm{HEM}_{11L}} = 38.63\mathrm{GHz}$, $Z_{\mathrm{int}}^{\mathrm{TM}_{01}} = 374\Omega$, $Z_{\mathrm{int}}^{\mathrm{HHEM}_{11L}} = 1.61k\Omega$, and it was assumed that the electrons have a vanishingly small velocity spread. The interaction length was chosen so that the interaction reaches saturation at the end of the structure when the asymmetric mode is turned "off". The simulation is terminated if one particle reaches the internal radius of the structure; the location where this occurs is denoted by $z = z_t$. As revealed by these frames, two facts are evident. Firstly, when the HEM_{11L} mode is turned on, the simulation is terminated before the end of the structure. Accordingly, the interaction process is less efficient than the case when the HEM_{11L} mode is turned off. Secondly if the guiding magnetic field is very strong (1.5T), the impact of the HEM_{11L} mode is still considerable. In conclusion, the impact of the HEM_{11L} mode on the transverse motion of the beam is critical for uniform beam ($\sim$50% variation).

The next step in the analysis of the system's performance is to check how the power level of the HEM_{11L} mode at the input end affects the beam expansion. Figure 4 illustrates the

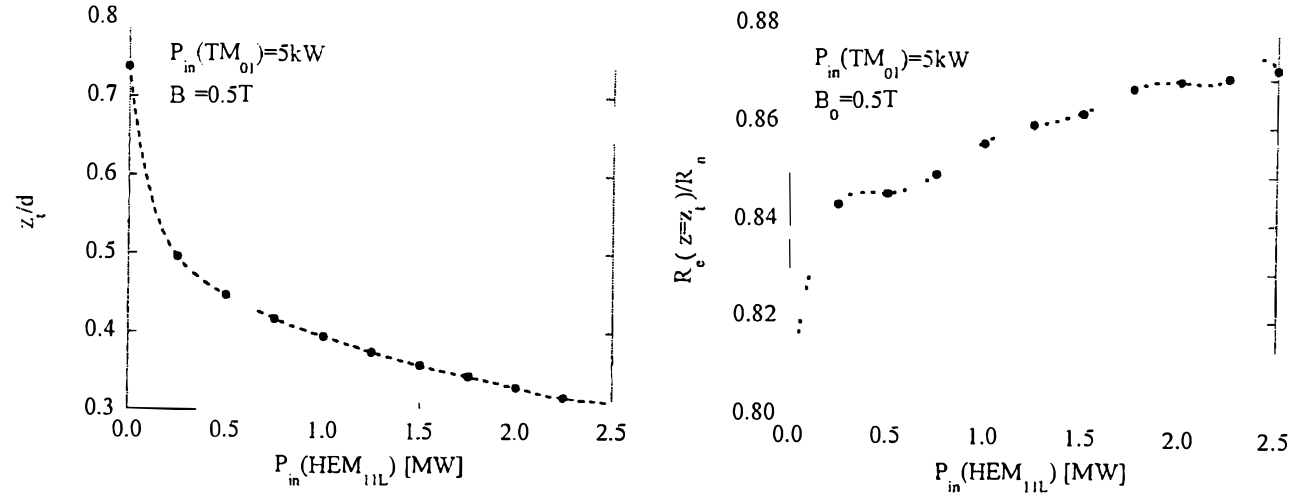

Figure 4: *Left*: The normalized termination point as a function of the initial power level of the HEM_{11L} mode at the input end. *Right*: The effective radius of the beam's envelope versus the HEM_{11L} mode power level at the input end.

beam expansion, when the power level of the asymmetric mode varies at the input end. At the left frame the effective interaction length is presented. At the right frame the radius of the beam's envelope is shown as a function of the HEM_{11L} mode power level at the input end. As one may expect this radius increases when increasing the input power as well as the effective interaction length does. In this simulation the parameters were used are identical to those used before.

It is evident from the former results that the HEM_{11L} mode plays a destructive role during the interaction process. For suppression of the HEM_{11L} mode, *selective* damping may be introduced i.e., that is a damping mechanism that is transparent to TM_{01} mode [7,8]. This type of damping may be accomplished by a series of choked loaded cavities [9]. These have high quality factor (Q) at the frequency that corresponds the TM_{01} mode and low Q otherwise.

In order to illustrate the potential of a series of a choked loaded cavities for the suppressing purpose, an "open cavity" with stub tuner was examined. For this example symmetric modes were only considered, thus using SUPERFISH to calculate the first four resonances and corresponding quality factor; the electric field distribution at 34.826GHz is illustrated in Figure 5. The quality factor at 34.826GHz was found to be 1720 whereas at three other eigen frequencies, 11.062, 22.792 and 44.377GHz, the quality factor is at least one order of

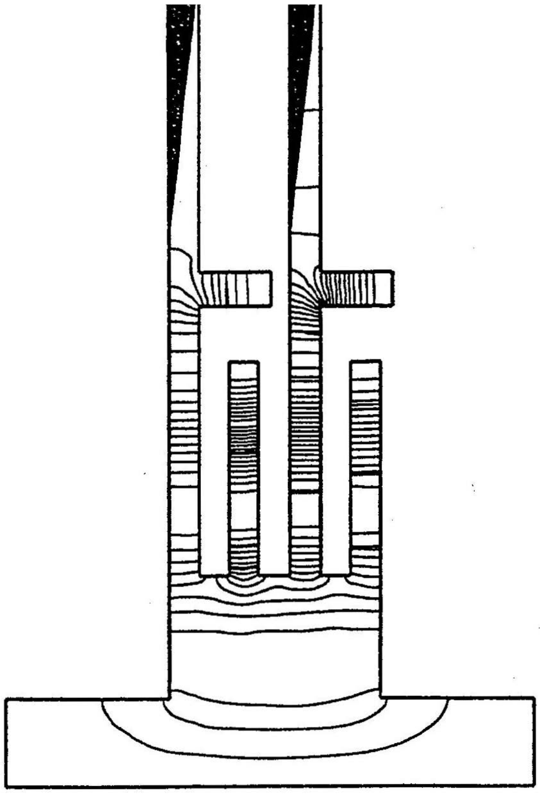

Figure 5: SUPERFISH simulation of a set of choked loaded cavities used to form a periodic structure (periodicity of 1.8mm, disk-thickness of 0.9mm, phase advance per cell of $\pi/2$, internal radius of 6mm and stub of 2.2mm). The system is designed to operate at 35GHz.

magnitude smaller, namely 60,72 and 112 correspondingly. Although these are only symmetric TM modes, a similar behavior for non-symmetric modes is anticipated. The advantages of such a way of suppression that it provides local suppression.

CONCLUSIONS

In conclusion, the design of high-power, high-efficiency traveling-wave amplifier should account for the effect of the asymmetric modes that the beam may interact with. A 3D model was developed for the investigation of the impact of asymmetric modes on the interaction process in particular the efficiency and the particles' dynamics. It was shown that substantial power associated with the HEM_{11L} mode accumulates in the structure, it may cause deflection of the beam to the wall. Finally a way to suppress asymmetric modes was suggested.

References

[1] S. Naqvi *et. al*; "High efficiency TWT Design Using Traveling Wave Bunch Compression", *IEEE Trans. on Plasma Science,* **26**, 3 p. 840, (1998).

[2] S. Banna; "The Interaction of Symmetric and Asymmetric Modes with free Electrons", *Research Thesis, Technion -Israel Institute of Technology*, Haifa (1999).

[3] P. Wang *et. al*; "A comparative Study of High Power, Multistage TWT Amplifiers", *Proc. of 1999 Particle Accelerator Conference*, New York p. 3600, (1999).

[4] W.K.H. Panofsky and W.A. Wenzel; "Some Consideration Concerning the Transverse Deflection of Charged Particles in Radio Frequency Fields, *Rev. Sci. Instr.* **27**, p. 967, (1956).

[5] H. Hahn; "Deflection Mode in Circular Iris-Loaded Wave-guide",*Rev. Sci. Instr.* **34**, p. 1094, (1963).

[6] H. Deruyter *et. al*; "Damped Accelerator Structures", *SLAC Pub.* p. 5263, (1990).

[7] S. Banna *et. al*; "The Interaction of Symmetric and Asymmetric Modes in High-Power Traveling-Wave Amplifier", *IEEE Trans. Plasma Science Special Issues.*

[8] L. Schächter, S. Banna and J. A. Nation; "Requirements of a High-Power TWT Operating at 35GHz"; *Advanced Acceleration Concepts AAC'98*, Baltimore, 1998.

[9] T. Shintake; "The Choke Mode Cavity", *Jpn. J. Appl. Phys.* **31**, p. 1567, (1992).

The *Center for Communication and Information Technologies* (CCIT)

is managed by the Department of Electrical Engineering.

This Technical Report is listed also as

EE PUB #1259, September 2000.